

## Microwave-Enhanced Reaction Rates for Nanoparticle Synthesis

Jeffrey A. Gerbec, Donny Magana, Aaron Washington, and Geoffrey F. Strouse\*

Contribution from the Department of Chemistry and Biochemistry, Florida State University, Tallahassee, Florida 32306-4390, and Mitsubishi Chemical Center for Advanced Materials, University of California, Santa Barbara, California 93106-9510

Received April 15, 2005; E-mail: Strouse@chem.fsu.edu

**Abstract:** Microwave reactor methodologies are unique in their ability to be scaled-up without suffering thermal gradient effects, providing a potentially industrially important improvement in nanocrystal synthetic methodology over convective methods. Synthesis of high-quality, near monodispersity nanoscale InGaP, InP, and CdSe have been prepared via direct microwave heating of the molecular precursors rather than convective heating of the solvent. Microwave dielectric heating not only enhances the rate of formation, it also enhances the material quality and size distributions. The reaction rates are influenced by the microwave field and by additives. The final quality of the microwave-generated materials depends on the reactant choice, the applied power, the reaction time, and temperature. CdSe nanocrystals prepared in the presence of a strong microwave absorber exhibit sharp excitonic features and a QY of 68% for microwave-grown materials. InGaP and InP are rapidly formed at 280 °C in minutes, yielding clean reactions and monodisperse size distributions that require no size-selective precipitation and result in the highest out of batch quantum efficiency reported to date of 15% prior to chemical etching. The use of microwave (MW) methodology is readily scalable to larger reaction volumes, allows faster reaction times, removes the need for high-temperature injection, and suggests a specific microwave effect may be present in these reactions.

### Introduction

The reports on new applications and technology for nanoscale semiconducting<sup>1–6</sup> and metallic<sup>7,8</sup> nanoparticles has grown in the past decade due to advancements in the chemical synthetic methodologies for their preparation. These materials are being utilized in applications including biomarkers,<sup>9–11</sup> solar cells,<sup>12–14</sup> and lighting technologies, for example. As the area of nanoscale devices becomes more of a commercial reality, the industrialization of nanoscale materials is realistically limited by the need for new material compositions and the development of high-throughput automation for materials preparation. For large-scale

reactions inhomogeneities in the growth process can be magnified by thermal gradients in the reaction which produce poor nucleation processes and therefore broadened size distributions. The inhomogeneity of large-scale reactions can be traced to the inefficient transfer of thermal energy from the heat source.

The growth of nanomaterials is dependent on the thermodynamic and kinetic barriers in the reaction as defined by the reaction trajectory and influenced by vacancies, defects, and surface reconstruction events. For the most part, the synthetic methods utilize conventional convective heating due to the need for high-temperature initiated nucleation followed by controlled precursor addition to the reaction. Conventional thermal techniques rely on conduction of blackbody radiation to drive the reaction. The reaction vessel acts as an intermediary for energy transfer from the heating mantle to the solvent and finally to the reactant molecules. This can cause sharp thermal gradients throughout the bulk solution and inefficient, nonuniform reaction conditions. This is a common problem encountered in chemical scale-up and is made more problematic in nanomaterials where uniform nucleation and growth rates are critical to material quality. New approaches for synthesis have been sought particularly for controlled growth. Recent synthetic advancements have included the use of nonsolvents and simpler reactants,<sup>15,16</sup> the use of single-source precursors,<sup>2,17,18</sup> and

\* To whom correspondence should be addressed at Florida State University.

- (1) Murray, C. B.; Norris, D. J.; Bawendi, M. G. *J. Am. Chem. Soc.* **1993**, *115*, 8706–8715.
- (2) Cumberland, S. L.; Hanif, K. M.; Javier, A.; Khitrov, G. A.; Strouse, G. F.; Woessner, S. M.; Yun, C. S. *Chem. Mater.* **2002**, *14*, 1576–1584.
- (3) Malik, M. A.; O'Brien, P.; Revaprasadu, N. *Chem. Mater.* **2002**, *14*, 2004–2010.
- (4) Jun, Y. W.; Choi, C. S.; Cheon, J. *Chem. Commun.* **2001**, 101–102.
- (5) Micic, O. I.; Curtis, C. J.; Jones, K. M.; Sprague, J. R.; Nozik, A. J. *J. Phys. Chem. B* **1994**, *98*, 4966–4969.
- (6) Talapin, D. V.; Rogach, A. L.; Mekis, I.; Haubold, S.; Komowski, A.; Haase, M.; Weller, H. *Colloids Surf. A* **2002**, *202*, 145–154.
- (7) Hyeon, T. *Chem. Commun.* **2003**, 927–934.
- (8) Xue, Z. L.; Terepka, A. D.; Hong, Y. *Nano Lett.* **2004**, *4*, 2227–2232.
- (9) Larson, D. R.; Zipfel, W. R.; Williams, R. M.; Clark, S. W.; Bruchez, M. P.; Wise, F. W.; Webb, W. W. *Science* **2003**, *300*, 1434–1436.
- (10) Gao, X. H.; Chan, W. C. W.; Nie, S. M. *J. Biomed. Opt.* **2002**, *7*, 532–537.
- (11) Fan, H. Y.; Yang, K.; Boye, D. M.; Sigmon, T.; Malloy, K. J.; Xu, H. F.; Lopez, G. P.; Brinker, C. J. *Science* **2004**, *304*, 567–571.
- (12) Cava, R. J.; et al. *Prog. Solid State Chem.* **2002**, *30*, 1–101.
- (13) Nozik, A. J. *Physica E* **2002**, *14*, 115–120.
- (14) Huynh, W. U.; Dittmer, J. J.; Libby, W. C.; Whiting, G. L.; Alivisatos, A. P. *Adv. Funct. Mater.* **2003**, *13*, 73–79.

- (15) Peng, Z. A.; Peng, X. G. *J. Am. Chem. Soc.* **2001**, *123*, 183–184.
- (16) Battaglia, D.; Peng, X. G. *Nano Lett.* **2002**, *2*, 1027–1030.
- (17) Revaprasadu, N.; Malik, M. A.; Carstens, J.; O'Brien, P. *J. Mater. Chem.* **1999**, *9*, 2885–2888.
- (18) Malik, M. A.; Revaprasadu, N.; O'Brien, P. *Chem. Mater.* **2001**, *13*, 913–920.

microfluidic reactors.<sup>8,19,20</sup> Even the use of household microwave ovens has been used to form nanoparticles,<sup>21–25</sup> although the crystallinity and optical properties appear to be lower in these systems.

Microwave heating methods can address the problem of heating inhomogeneity, while providing a scalable platform for industrial applications. In fact, microwave heating has been demonstrated to enhance reaction rates, selectivity, and product yields in organic chemistry.<sup>26</sup> By judicious choice of the solvents, passivating ligands, and reactants, the nanomaterial precursors can be selectively heated preferentially with regards to the solvent or passivating ligand. Selective heating in the microwave cavity is advantageous in organic synthesis, and in general these microwave synthetic methodologies are quite adaptable to reactions that have high energies of activation and slow reaction rates.<sup>27,28</sup> This effect alone has advantages for colloidal nanostructured materials synthesis.

In this paper, we describe the development of microwave synthetic methodology and the influence of additives for a range of organically passivated binary and ternary III–V (InGaP, InP) and II–VI (CdSe) materials. The nanomaterials are reproducibly prepared in less than 20 min in a focused 2.45 GHz, single-mode high-power microwave (300–400 W/cm<sup>2</sup>) capable of operating at 300 °C for extended reaction times. The as-prepared materials are crystalline with a size distribution of 5–6% and spherical in shape. Exploration of the power, temperature, time, and additive dependent growth is investigated. Microwave chemistry appears to enhance reaction rates either by overcoming local intermediates which act as traps along the reaction trajectory or by increasing the microscopic temperature of the reaction. The difference in the effect of additives and the microwave variables (temperature, time, and power) for the II–VI and III–V materials suggest that local intermediates and transition states in the reaction trajectory are substantially different. The III–V materials show no time, temperature, or power dependent growth in the microwave; however when the typical high-boiling noncoordinating solvent, octadecene (ODE), is replaced with a low boiling solvent, decane, the colloidal size distribution is significantly narrowed and the quantum efficiencies are increased (QY = 15%) presumably due to increased reaction pressures that may anneal out vacancy or defects in the forming nanocrystals. CdSe growth and properties are dependent on the addition of ionic liquids, as well as reaction

temperature in concert with the applied microwave power and reaction time.

## Experimental Section

The reactants were purchased from Aldrich Chemical and used without further purification if not otherwise stated. Decane was purified previously by distillation over activated 4 Å molecular sieves. Isolation of all nanomaterials is achieved under an Ar atmosphere by dissolution of the room-temperature reaction mixture in a minimum of toluene, addition of a 2:1 anhydrous butanol/methanol solution to induce particle precipitation, and collection of the solid via centrifugation. The process is repeated 3 times to remove unwanted reactants. All glassware was dried prior to use.

Microwave nanoparticle synthesis<sup>33</sup> was carried out in a modified CEM Discover microwave using single mode and continuous power at 2.45 GHz. Although the reactions can be carried out in any microwave, reaction temperature, microwave power, and mode quality are critical in producing the highest structural, size dispersity, and optical quality. The CEM microwave cavity was commercially modified by CEM with a Teflon insert to allow sustainable heating at 300 °C at powers up to 400 W. Each example reaction was carried out in a sealed reaction vessel with 5 mL of the respective starting solution. To maintain stable power and temperature during the reaction, the microwave cavity was actively cooled by compressed air to remove latent heat from the reaction. Active cooling via compressed air allows higher powers to be applied without increasing the reaction temperature. It should be noted that the use of compressed air results in thermal gradients from the reaction vessel inward toward the reaction center. Reaction temperatures are measured at the vessel wall in the microwave, which will mean that the actual microscopic reaction temperature is not measured; rather the average vessel temperature is reported.

Initiation of the reaction is carried out at maximum power to achieve a desired reaction temperature as rapidly as possible. During the growth phase for nanocrystal chemistry the power and reaction temperature were varied to maximize the quality of the individual materials as measured by transmission electron microscopy (TEM), powder X-ray diffraction (pXRD), and optical absorption and photoluminescence (PL). The results of the growth-phase studies suggest the temperature and power parameters are unique to the material type but dictate material quality in the microwave reactions for all nanomaterials studied.

**Preparation of CdSe by Li<sub>4</sub>[Cd<sub>10</sub>Se<sub>4</sub>(SPh)<sub>16</sub>].** The CdSe was prepared using the single-source precursor Li<sub>4</sub>[Cd<sub>10</sub>Se<sub>4</sub>(SPh)<sub>16</sub>]<sup>2</sup>. The additive study with an ionic liquid was carried out using a stock solution of the precursor cluster prepared by adding 635 mg of Li<sub>4</sub>[Cd<sub>10</sub>Se<sub>4</sub>(SPh)<sub>16</sub>] and 0.0448 g of 1-hexyl-3-methylimidazolium chloride to 45 g of degassed 1-aminohexadecane (HDA) at 90 °C. The solution was degassed under Ar, and 5 mL aliquots were injected into the microwave reaction vials prior to the reaction. Sample quality for all reactions was monitored by absorption spectroscopy, photoluminescence (PL) and pXRD.

**Preparation of CdSe by CdO.** To investigate other reactions and the effect of a strong microwave absorber (trioctylphosphine oxide, TOPO), the microwave studies were carried out using CdO and tetrabutyl phosphine selenide (TBPSe) as precursors by the method of Qu and Peng.<sup>29</sup> The Cd and Se precursors were prepared according to literature methods in a mixture of 50:50 (w/w) HDA (1-aminohexadecane) and TOPO as the solvent.<sup>29</sup> The Se precursor was injected into the Cd solution at 50 °C and mixed for 15 min. The solution was maintained at 50 °C to allow the reactants to remain in the liquid state for transfer into the microwave reaction vials. The ramping power was set to 300 W until the desired reaction temperature was reached. At this time active cooling was employed to maintain a high power density at 280 W for the duration of the reaction. Each reaction time consisted of a duration of 30 s. The ramping period ranged from 30 s to 1 min,

- (19) Chan, E. M.; Mathies, R. A.; Alivisatos, A. P. *Nano Lett.* **2003**, *3*, 199–201.
- (20) Wang, H. Z.; Li, X. Y.; Uehara, M.; Yamaguchi, Y.; Nakamura, H.; Miyazaki, M. P.; Shimizu, H.; Maeda, H. *Chem. Commun.* **2004**, 48–49.
- (21) Verma, S.; Joy, P. A.; Khollam, Y. B.; Potdar, H. S.; Deshpande, S. B. *Mater. Lett.* **2004**, *58*, 1092–1095.
- (22) Bensebaa, F.; Zavaliche, F.; L'Ecuyer, P.; Cochrane, R. W.; Veres, T. J. *Colloid Interface Sci.* **2004**, *277*, 104–110.
- (23) Rogach, A. L.; Nagesha, D.; Ostrander, J. W.; Giersig, M.; Kotov, N. A. *Chem. Mater.* **2000**, *12*, 2676–2685.
- (24) Zhu, J. J.; Palchik, O.; Chen, S. G.; Gedanken, A. *J. Phys. Chem. B* **2000**, *104*, 7344–7347.
- (25) Murugan, A. V.; Sonawane, R. S.; Kale, B. B.; Apte, S. K.; Kulkarni, A. V. *Mater. Chem. Phys.* **2001**, *71*, 98–102.
- (26) Gedye, R. N.; Wei, J. B. *Can. J. Chem.* **1998**, *76*, 525–532.
- (27) Guzelian, A. A.; Katari, J. E. B.; Kadavanich, A. V.; Banin, U.; Hamad, K.; Juban, E.; Alivisatos, A. P.; Wolters, R. H.; Arnold, C. C.; Heath, J. R. *J. Phys. Chem. B* **1996**, *100*, 7212–7219.
- (28) Heath, J. R.; Shiang, J. J. *Chem. Soc. Rev.* **1998**, *27*, 65–71.
- (29) Qu, L. H.; Peng, X. G. *J. Am. Chem. Soc.* **2001**, *124*, 2049–2055.
- (30) Strouse, G. F.; Gerbec, J. A.; Magana, D. Method for Synthesis of Colloidal Nanoparticles. Patent Pending 2005, S/N 10/945, 053.
- (31) Lidstrom, P.; Tierney, J.; Wathey, B.; Westman, J. *Tetrahedron* **2001**, *57*, 10229–10229.
- (32) Loupy, A. *Microwaves in Organic Synthesis*; Wiley-VCH: Weinheim, Germany, and Cambridge, U.K., 2002.

- (33) Thostenson, E. T.; Chou, T. W. *Composites, Part A* **1999**, *30*, 1055–1071.

depending on the reaction temperature. Sample quality for all reactions was monitored by absorption spectroscopy, photoluminescence (PL), and pXRD.

**Preparation of InGaP in Octadecene.** The preparation of InGaP is based on a modification of literature methods.<sup>16,30</sup> The In and Ga intermediates were prepared by mixing 2.71 mmol of indium(III) acetate and 0.271 mmol of gallium(III) 2,4-pentanedionate and 8.94 mmol of hexadecanoic acid with 190 mL of ODE in a three-neck flask. The cation intermediates were formed by heating the solution to 110 °C under vacuum for 2 h with four cycles of Ar backfilling. The temperature of the solution was allowed to cool to 50 °C at which time 1.50 mmol of tris(trimethylsilyl)phosphine was injected (TMSP). The In/Ga/P precursor solution immediately turned from colorless to yellow. The In/Ga/P precursor solution was kept under Ar at 50 °C as a stock solution for later use. For a typical reaction, 5 mL of the stock solution was removed by Teflon syringe and placed in a reaction tube (CEM Corp.). The ramp period was set to 300 W to achieve the reaction temperature in the least amount of time. Once the desired reaction temperature was reached, the active cooling was employed by stabilizing the power at 280 W by applying compressed air (~3–7 psi) to the reaction vessel. Once the reaction was complete, the power was reduced to 0 W and the compressed air flow was increased to 70 psi for maximum cooling. Sample quality for all reactions was monitored by absorption spectroscopy, PL, and pXRD (Supporting Information Figure 1). In addition, TEM was measured on the InGaP samples to measure their shape and crystallinity (Supporting Information Figure 2).

**Preparation of InGaP in Decane.** The reaction stoichiometry and method in decane is identical to the reaction in ODE. The preparation of the cations consisted of placing 710  $\mu\text{mol}$  of indium(III) acetate and 74.1  $\mu\text{mol}$  of gallium(III) 2,4-pentanedionate and 2.36 mmol of hexadecanoic acid in a three-neck flask. The cations (In/Ga) were prepared in the absence of the noncoordinating solvent due to its low boiling point (174 °C). This was achieved by heating the salts to 150 °C under reduced pressure. The melt was clear and colorless and was backfilled with Ar four times at this temperature. The reactants were allowed to cool to room temperature at which time 50.0 mL of decane was injected into a flask under inert conditions. The temperature was raised to 50 °C to afford a clear and colorless solution at which time 393  $\mu\text{mol}$  of tris(trimethylsilyl)phosphine was injected. The solution slowly turned pale yellow over a 30 min time period. A 5 mL aliquot of the stock solution was placed in microwave reaction tubes and immediately placed in the microwave chamber for various reaction times (from 30 s to 7 min) at 280 °C with a stable power at 280 W by active cooling. The ramping and cooling parameters were identical to the InGaP prepared in octadecene. Sample quality for all reactions was monitored by absorption spectroscopy, PL, and pXRD.

**Preparation of InP in Octadecene.** The InP nanomaterials are prepared in the same manner as InGaP prepared in octadecene, keeping the cation/anion mole ratio at 2:1 and the cation/ligand mole ratio at 1:3, and maintained at 50 °C under Ar. A 78.5  $\mu\text{mol}$  amount of 1-hexyl-3-methylimidazolium chloride, trihexyltetradecylphosphonium decanoate, and trihexyltetradecylphosphonium bromide were massed into separate microwave reaction vials inside an Ar-filled drybox and sealed to later be taken into the fume hood. A 5 mL aliquot of the InP stock solution was injected into the microwave reaction tubes prior to each reaction. The sample quality for all reactions was monitored by absorption spectroscopy, PL, and pXRD.

## Results and Discussion

Microwave chemistry has become a widely used synthetic methodology in organic chemistry that takes advantage of the selective nature of microwave heating for materials that have high dielectric losses, namely, polar systems.<sup>31</sup> Dielectric heating in contrast to convective heating, heats the total volume of the reactants by transferring energy selectively to microwave

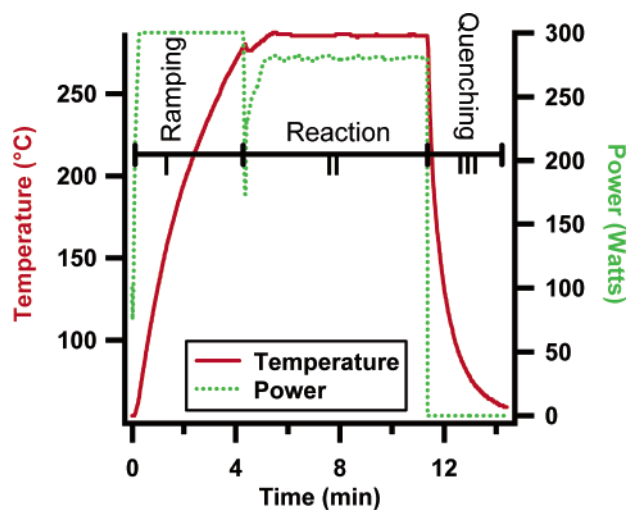


**Figure 1.** Temperature (°C) and power (W) profiles of a typical InGaP reaction. Region I shows the temperature ramp carried out at 300 W until the desired temperature is reached (280 °C). During the reaction time (II), the power and temperature are maintained at 280 °C and 280 W. Once the reaction is complete, the reaction is thermally quenched by compressed air.

absorbing materials. The larger the microwave cross-section for a particular constituent, the more dramatic the heating process is. It can therefore be imagined that the intrinsic temperature localized around the ions is significantly higher in temperature than that of the bulk solution. Because precursors and intermediates along a given reaction trajectory can have different dielectric constants, microwaves can be used to overcome high activation energies for product formation by selectively coupling to intermediates in the transition states. In organic chemistry the better understanding of the reaction trajectories leads to the so-called “specific microwave effect” to systematically manipulate the products generated from a given reaction.<sup>32</sup> In organic reactions, the nature of the selective heating of microwave absorbing materials therefore allows both rapid heating rates and high temperatures to be reached which in turn drive chemical reactions. In addition, it is established that volumetric heating with microwaves reduces the overall thermal gradients in the reaction, producing a more uniform product formation. For nanocrystal growth the higher reaction temperatures, greater thermal control, and lower thermal gradients are needed to produce high-quality materials.<sup>33,34</sup> If the inorganic precursor or the forming nanoparticle has a higher cross-section for microwave absorption relative to the reaction solvent, higher reaction temperatures will be achieved in comparison to convective heating with the solvent acting as a thermal mediator absorbing energy from the reactants rather than transferring the heat to the reaction. This suggests if the nanoparticle or intermediates are selectively heated relative to the solvent, that the temperature of the reaction in the microwave, measured at the vessel and/or solvent, can be potentially much higher. This provides exquisite control over the reactions by providing temperature, time, microwave power, and absorption cross-section as mediators for materials synthesis.

Figure 1 illustrates a typical reaction trajectory for a nanomaterial grown in a nonpolar solvent. The microwave reaction can be divided into three reaction stages: temperature ramping

(34) Jones, D. A.; Lelyveld, T. P.; Mavrofidis, S. D.; Kingman, S. W.; Miles, N. J. *Resour., Conserv. Recycl.* **2002**, *34*, 75–90.

or instantaneous heating to initiate nucleation; a growth regime manipulated by reaction time and temperature; and a rapid thermal quenching step to control Ostwald ripening (reaction termination). In the microwave, the nucleation process is achieved by rapidly increasing the temperature from room temperature (RT) to 280 °C at full microwave power (300–400W). During the growth phase the power is reduced to maintain a controlled growth stage. The temperature of the reaction is held constant by active cooling of the reaction vessel with forced air to allow power and temperature to be controlled independently. The drawback of active cooling is thermal gradients may be higher than measured. Active cooling carries latent heat away from the vessel during the reaction to stabilize the applied power at a given reaction temperature, allowing a high power density to be applied to the reaction constituents. In this case it is probable that there is an inside-out thermal gradient in which the highest temperature is found near the center of the solution.

Reaction times are based upon the time at a desired temperature and are chosen according to the desired reaction and nanomaterial size. Once the reaction is complete, the microwave power is turned off to terminate the reaction and the air flow is increased to rapidly cool the solution, quenching the reaction which minimizes colloidal size distributions resulting from Ostwald ripening. All three stages in the microwave are critical in the formation of a narrow size distribution of colloids with high optical qualities as measured by absorption and photoluminescence and will be discussed separately below.

**Initiation Phase.** The quality of the final nanomaterials is dependent on the initiation of the reaction. It has been suggested that uniformity in heating, introduction of the precursor, and controlled temperature over the course of the reaction are crucial to final product quality.<sup>35–37</sup> In standard lyothermal synthetic methods, this tends to be achieved by rapid injection of the precursors at high temperature with the solvent acting to provide the convective heat. To eliminate out-of-control growth in the lyothermal synthesis, the innate cooling of the reaction upon injection of a cold reactant controls the growth phase, although reactant concentration and activity are also important. In the microwave, we believe nanoparticle formation and growth is initiated by selective microwave heating of constituents in the reaction. The selective heating can either be to the precursors or to an organic constituent in the reaction depending on the reaction type. In either case the local temperature is elevated and forms a uniform thermal field. This in turn must provide energy to drive the desired product by overcoming transition states in the reaction trajectory. Unfortunately, while in organic chemistry the microwave dependent effects can be specifically discussed in terms of the reaction trajectory, the lack of an in-depth mechanistic picture for nanoparticle growth makes determination of the exact influence of the microwave on the transition states for nanoparticle formation to be unclear.

The influence on the product formation under microwave heating will depend on the applied microwave power ( $P$ ) and the competitive microwave cross-section of the reactants and

passivants in solution, as measured by the heating rate. This of course will be dependent on the microwave cavity design, but the general observations will be relevant to all designs. The heating rate ( $dT/dt$ ) in a microwave reactor correlates with the real ( $\epsilon'$ ) and imaginary ( $\epsilon''$ ) components of the complex dielectric constant ( $\epsilon^*$ ) for the individual components in the reaction mixtures. The microwave absorption cross-section is described by the real component while the ability to transfer microwave energy into heat is described by the loss tangent ( $\tan \delta = \epsilon''/\epsilon'$ ).<sup>33</sup> Molecules with large permanent dipoles will absorb microwave irradiation selectively over molecules with small dipoles. The magnitude of the microwave absorption cross-section is therefore dependent on the materials dielectric constant or permittivity ( $\epsilon'$ ). This value tends to be small for nonpolar organic moieties ( $\sim 2.0$  for benzylic molecules) and values of up to 80 for water.<sup>33</sup>

Since selective heating in the microwave requires a large dipole, the rate of heating of the reactants in an applied electric field ( $E$ ) is described by

$$dT/dt = \sigma[E]^2/\rho C \quad (1)$$

where  $\rho$  is the density and  $C$  is the specific heat capacity of the molecule, and the molecular conductivity ( $\sigma$ ) is related to the imaginary part ( $\epsilon''$ ) of the permittivity function using a Debye relationship,  $\epsilon^* = \epsilon' + i\epsilon''$ .<sup>33</sup> In general the value of  $E$  is dependent on the cavity design, and therefore not calculable; however the expression indicates that initiation of the nanomaterial reaction is controllable by the dielectric constant of the reactants and therefore the heating rate of the reaction. The temperature ramping depends on the ability of each of the constituent elements in the reaction to absorb microwaves ( $\epsilon$ ) and the solvent thermal conductivity.

The element in the reaction mixture that couples with the microwaves the strongest will give rise to the major component of the heat transfer. If the element is a transition-state intermediate along the reaction path, it can assist in product formation. If the element is a polar or ionic species, including organic salts or ionic liquids, not involved in the transition states, they will contribute to an average increase in the overall reaction temperatures which can also be advantageous.<sup>38,39</sup>

In the microwave, interpretation of heating rates is complicated by the fact that the temperature is a measure at the reaction vessel and is not a direct reflection of the microscopic reaction temperature. Inspection of the rates does provide insight into the effects of additives to reactions and therefore can provide insight into how to control reaction trajectories. In Figure 2, the effect of solvent and reactant choice on reaction heating rates is illustrated for a series of reactions for CdSe at 400 W and InP and InGaP at 300 W. In the CdSe reactions, it is clear in Figure 2A the heating rates for the reactions with CdSe/HDA/IL (IL = ionic liquid; 12 °C/s) and with TOPO/HDA/CdO (9 °C/s) are enhanced relative to heating pure HDA (3 °C/s) or the reaction CdSe/HDA (4 °C/s). The deviation at 62 °C for the HDA and CdSe/HDA curves in Figure 2A arise from melting of the HDA (1-aminohexadecane). Upon addition of the ionic liquid 1-hexyl-3-methylimidazolium chloride, the heating rate of the solution increases dramatically due to the large microwave

(35) Peng, X. G.; Wickham, J.; Alivisatos, A. P. *J. Am. Chem. Soc.* **1998**, *120*, 5343–5344.

(36) Murray, C. B.; Kagan, C. R.; Bawendi, M. G. *Annu. Rev. Mater. Sci.* **2000**, *30*, 545–610.

(37) Talapin, D. V.; Kornowksi, A.; Haase, M.; Weller, H. *J. Am. Chem. Soc.* **2002**, *124*, 5782–5790.

(38) Leadbeater, N. E.; Torenius, H. M. *J. Org. Chem.* **2002**, *67*, 3145–3148.

(39) Antonietti, M.; Kuang, D. B.; Smarsly, B.; Yong, Z. *Angew. Chem., Int. Ed.* **2004**, *43*, 4988–4992.

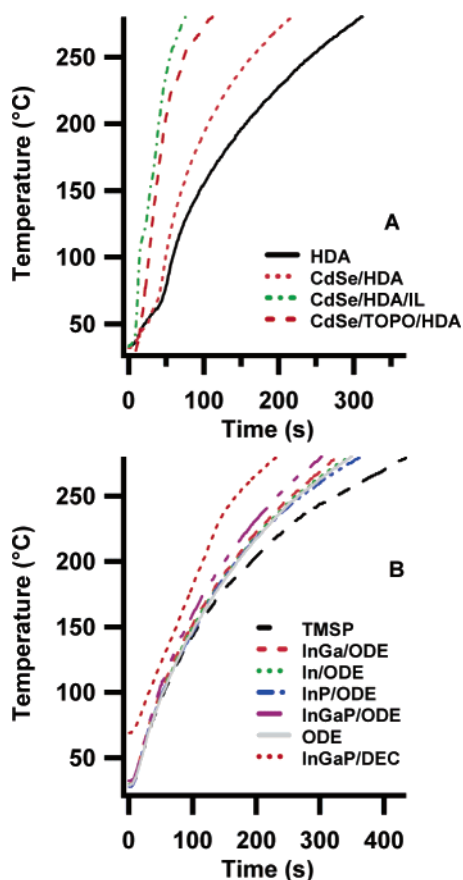


**Figure 2.** Temperature ramping rates for molecular precursors and solvents used in the formation of (A) CdSe at 400 W and (B) III–V nanoparticles at 300 W. In A, HDA is for 5 mL of hexadecylamine, the curve for CdSe/HDA is for a solution containing  $\text{Li}_4[\text{Cd}_{10}\text{Se}_4(\text{SPh})_{16}]$  dissolved in HDA, the curve CdSe/HDA/IL represents a solution containing  $\text{Li}_4[\text{Cd}_{10}\text{Se}_4(\text{SPh})_{16}]$  in HDA with the ionic liquid (IL) 1-hexyl-3-methylimidazolium chloride added, and the curve for TOPO/HDA/CdO is for a 50:50 (v/v) mixture of the solvents with CdO and TBPSe added. In B, TMSP represents a solution containing tris(trimethylsilyl)phosphine in octadecene; In/ODE and InGa/ODE represent solutions containing the metal salts in a mixture of hexadecanoic acid and ODE; and InP/ODE and InGaP/ODE represent identical solutions with TMSP added. The curve for ODE is for 5 mL of technical grade octadecene.

cross-section for ionic liquids, as previously observed in microwave-driven reactions.<sup>38</sup> Likewise, the large heating rate for TOPO/CdO is due to the high-absorption cross-section for TOPO. The effect of the ionic liquid and TOPO to rapidly heat the bulk solution can be traced back to their selective ability to couple with the microwaves and efficiently convert electromagnetic energy into heat. The effect of the higher heating rate in the presence of the ionic liquids will increase the microscopic reaction temperatures of the reaction. In turn these accelerated heating rates translate to rapid particle growth as discussed below.

The effect of reaction conditions on heating rates in the formation of InP and InGaP are less conclusive and are shown in Figure 2B. The rate of heating for the InP and InGaP reactions in ODE and decane are slow, 2 °C/s. The largely invariant heating rates observed for the different reaction conditions is not surprising when considering the polarizability of the group III precursors is small and the precursor concentrations are low in solution. The observation that ODE and decane show a heating rate of 2 °C/s identical to that of the InP and InGaP reactions suggest that only the solvent is absorbing the MW

energy. However, this assumption is incorrect since the actual microscopic temperature of the reaction may be substantially higher than that measured. The measured rate of solvent heating in Figure 2 is dictated by solvent thermal conductivity and thermal load on the solvent. In the case of nanoparticle growth without added ILs, the thermal load is likely to be small since the nanoparticles should thermalize rapidly due to their small size and exist in low concentration.

**Growth Phase.** During the growth phase for nanomaterials uniform volumetric heating is important to maintain the size focus. In the microwave, the reaction temperature is achieved by uniform volumetric heating, which is influenced by the power dissipation to the solvent and the applied power. The dissipation of power per unit volume ( $P$ ) is described by  $P = \sigma[E]^2$ , where  $\sigma$  is the conductivity and  $E$  is the applied electric field. The applied power influences the temperature of the reaction solution. The temperature of the reaction is mediated by thermal transfer of latent heat from the reactant to the solvent and dissipation by active air-cooling in the microwave. Excess heat will tend to drive Ostwald ripening processes in nanomaterial synthesis.

**CdSe Nanoparticle Formation.** The growth of CdSe nanoparticles is an ideal platform to compare the quality and the rate of growth for nanoparticles grown by convective heating and microwave heating methods. In the following discussion, we separate the influence of additives on the growth of CdSe from a single-source precursor route using  $\text{Li}_4[\text{Cd}_{10}\text{Se}_4(\text{SPh})_{16}]$  and added ionic liquids and the effect of having a solvent that is a strong microwave absorber (TOPO) using a CdO method developed by Qu and Peng.<sup>40</sup> The prepared materials, whether grown by convective method or by dielectric heating, are identical with similar absorption features, photoluminescence quantum yields, and similar size dispersities for a given reaction methodology. Significant differences exist between convective and dielectric heating with regard to material handling, where the reactants can be added at room temperature without the need for high-temperature injection to produce high-quality materials; for material growth, where the growth times even for III–V materials is under 15 min; and in increased reproducibility from reaction batch to reaction batch.

The influence of microwave power, reaction time, and reaction temperature is demonstrated for CdSe formed from  $\text{Li}_4[\text{Cd}_{10}\text{Se}_4(\text{SPh})_{16}]$  in Figure 3. In Figure 3A the influence of varying times (0–55 min) at fixed power (400 W) and fixed temperature (300 °C) is investigated. The effect of increasing reaction times past 10 min is minimal with regard to size (2 nm), as evidenced by the position of the first exciton feature. A change in size distribution is observed for distribution for times longer than 45 min as measured by PL shape and absorption bandwidth. Inspection of Figure 3B shows at a fixed reaction time (40 min) and microwave power (400 W) a dependence of size on temperature is clearly observed. The nanoparticle size increases with increasing temperature. Figure 3C demonstrates increasing the microwave power from 300 to 400 W for a reaction of 10 min at 210 °C does not have a marked effect on the nanomaterial size or the optical quality as measured by absorption excitonic features and photoluminescence. Lower powers are not presented due to the observation of slow heating rates, a difficulty to achieve the necessary

(40) Qu, L. H.; Peng, X. G. *J. Am. Chem. Soc.* **2002**, *124*, 2049–2055.

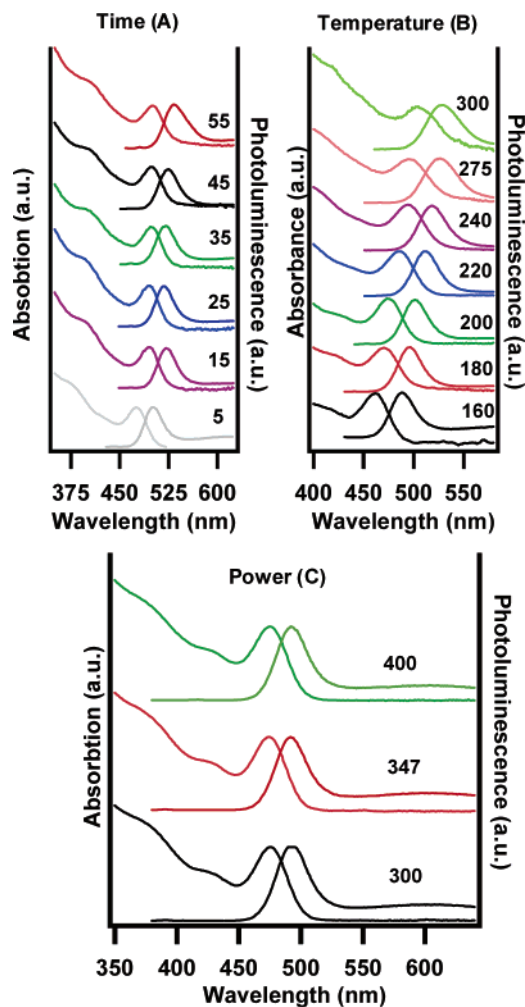


**Figure 3.** Room-temperature absorption and photoluminescence of toluene isolated CdSe nanoparticles grown from  $\text{Li}_4[\text{Cd}_{10}\text{Se}_4(\text{SPh})_{16}]$  synthesized at various (A) powers (W), (B) times (min), and (C) temperatures ( $^{\circ}\text{C}$ ). In these graphs, one parameter is varied while the other two parameters (time, power, or temperature) remain constant. The variables at which the reactions were carried out are indicated next to the trace.

reaction temperatures, and poor optical performance of the resultant materials.

The observation of small nanoparticles ( $\sim 2$  nm) even at high power, long reaction times, and high temperature is surprising given that convective heating allows 9 nm CdSe nanocrystals to be isolated after several hours of reaction time.<sup>2</sup> We believe this suggests local minima may exist in the reaction trajectory for growth of nanocrystalline CdSe from the precursor methods that require long reaction times to overcome. Local minima along a reaction trajectory may arise even for reactions that are thermodynamically downhill to bulk; however, due to reconstruction or kinetics may be slow to progress over their transition state to the final product. In fact, a surface reconstruction event coupled to surface passivation has been suggested by Yu et al.<sup>41</sup> Consistent with this observation, in a recent paper Burda et al. indicated a unique stabilization at 2 nm is observed in the growth of nanocrystalline CdSe.<sup>42</sup>

The addition of an ionic liquid (IL) to a reaction can increase reaction temperatures due to their strong microwave cross-

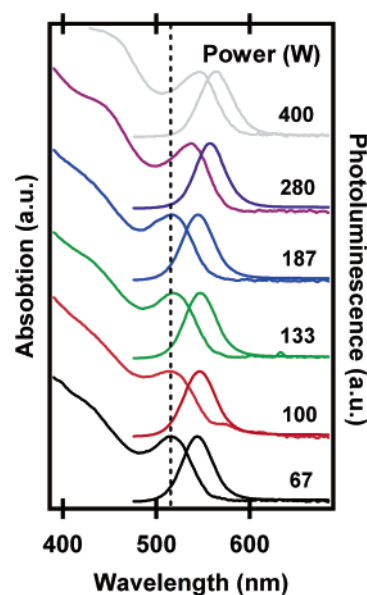


**Figure 4.** Power dependent (W) size characteristics of CdSe nanoparticles formed by microwave heating with ionic liquid addition (1-hexyl-3-methylimidazolium). The applied power was increased from 160 to 400 W, keeping the reaction time at 3 min and the reaction temperature fixed at  $210^{\circ}\text{C}$ .

section, can stabilize transition-state species, and can act as catalyst toward growth.<sup>43</sup> The observed heating rate differences in Figure 2 suggests that addition of ionic liquid to HDA in the formation of CdSe may increase the microscopic reaction temperature and in turn may influence nanoparticle growth. Addition of a strong microwave absorber to a reaction has been shown in microwave-assisted organic chemistry to increase the microscopic temperature of the reaction, overcome local minima, and push the reaction toward the thermodynamic product.<sup>44</sup> In Figure 4, it is clear that for CdSe nanoparticles grown in the presence of a 1.1 mole ratio of 1-hexyl-3-methylimidazolium chloride (IL) to the inorganic cluster, a large increase in nanoparticle size from 2 nm to greater than 5 nm in less than 10 min is observed. This is further shown in a direct comparison in Supporting Information Figure 3. A plot of the nanoparticle size versus reaction condition (Figure 5) shows a dependence on time, temperature, and power in the presence of the ionic liquid. At fixed temperature and time a steady growth is observed without a clear asymptote for size vs power, suggesting increasing power will increase size (Figure 5A). At fixed power and temperature (Figure 5B), the nanoparticle approaches an asymptote at  $\sim 3.5$  nm rapidly. At fixed power and time (Figure 5C) the growth is slow to initiate at temperatures below  $180^{\circ}\text{C}$  (3.0 nm), but shows steady growth between 180 and  $\sim 220^{\circ}\text{C}$  (5.5 nm). The lines in the figure provide a guide to the eye. It is clear that the addition of the IL results in a strong dependence on the reaction conditions, which was not previously observed. In addition the reaction rate is accelerated, suggesting that reaction barriers are overcome by heat transfer to the reactants mediated through the solvent or by displacing the amine passivating ligands, as has been observed when ODE is added as a nonpassivant to lyothermal synthesis<sup>15</sup>

(41) Yu, W. W.; Wang, Y. A.; Peng, X. G. *Chem. Mater.* **2003**, *15*, 4300–4308.

(42) Chen, X. S., A.; Lou, Y.; Burda, C. *J. Am. Chem. Soc.* **2005**, ASAP.

(43) Chiappe, C.; Pieraccini, D. *J. Phys. Org. Chem.* **2005**, *18*, 275–297.

(44) Eames, J.; Kuhnert, N.; Sansbury, F. H.; Warren, S. *Synlett* **1999**, 1211–1214.

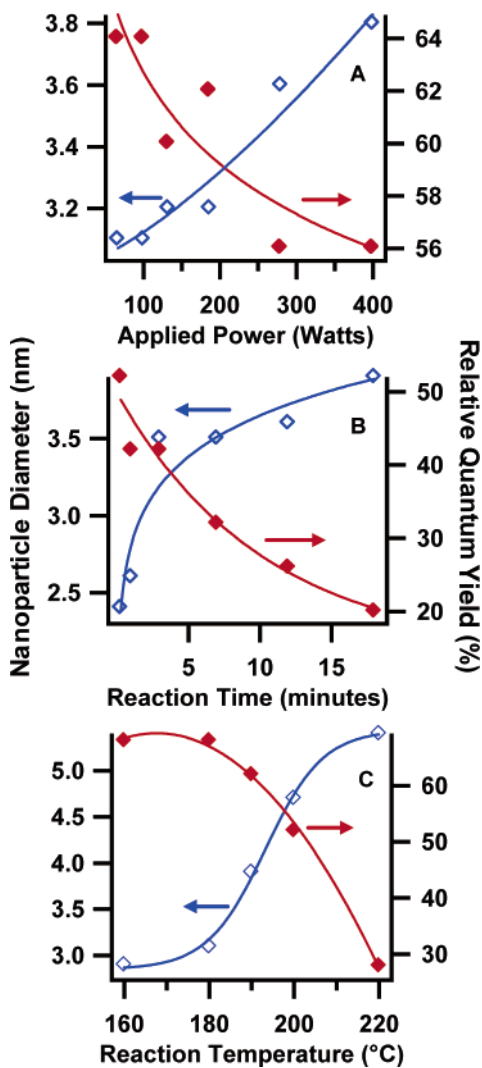


**Figure 5.** Nanoparticle diameter and quantum efficiency (QY) of CdSe synthesized at (A) various powers (W) at 3 min and 210 °C, (B) various times (min) at 100 W and 220 °C, and (C) various temperatures for 10 min at 220 W. The QY was measured at RT in a thin path configuration using a 4 mm × 10 mm quartz cuvette on a 10<sup>-8</sup> M solution of the nanoparticle in toluene relative to rhodamine R6G in ethanol at RT.

A plot of the change in QY with reaction condition appears in Figure 5. The measured QY<sup>45</sup> for the cluster-grown materials is within experimental error as a function of power (56–64%), but not for time (20–52%) and temperature (28–70%). In all cases, the QYs are experimentally similar for a given size, and the observed variance with time and temperature may reflect the larger change in size for these conditions. It is important to note that the maximum QY obtained for the single-source materials for a core-only nanocrystal achieved a reproducible maximum value of ~70% for a 5.5 nm dot (Figure 5C). Further changes in passivant and core shelling would allow QYs to be obtained at the same level as the best reported materials to date. Due to the high self-absorptivity of these materials, the QY measurements were conducted in thin path configurations

(45) The relative quantum efficiencies were obtained using the following expression,  $\phi_{em} = \phi'_{em}(I/I')(A'/A)(n/n')^2$ , where  $I$  (sample) and  $I'$  (reference) are integrated emission peak areas,  $A$  (sample) and  $A'$  (reference) are the absorbances at the excitation wavelength, and  $n$  (sample) and  $n'$  (reference) are the refractive indices of the solvents.  $\phi'_{em}$  is the quantum efficiency of the reference.

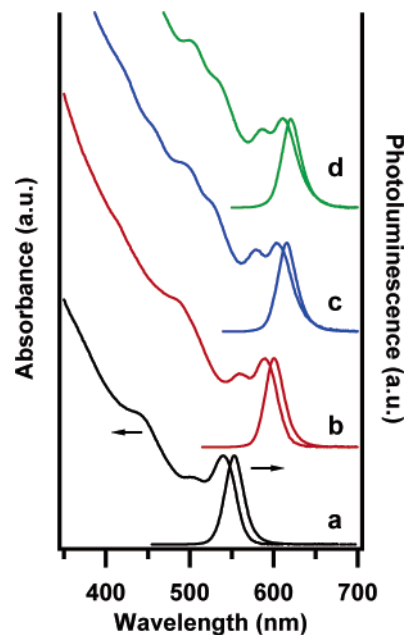


**Figure 6.** Absorption and photoluminescence in toluene of CdSe prepared in the microwave by CdO in hexadecylamine and triethylphosphine oxide. The reactions were carried out at (a) 200, (b) 240, (c) 280, and (d) 300 °C for 30 s at 160 W to achieve different sizes. No active cooling was applied.

analogous to methods applied for high-efficiency laser dyes as outlined in the Experimental Section.

Strong microwave absorbers in a reaction can drastically accelerate the rate of material formation. This is very evident upon inspection of the synthesis of CdSe from CdO in TOPO (triethylphosphine oxide). TOPO, which has a large static dipole, is a strong microwave absorber, as evidenced by the rapid heating rate observed in Figure 2. Figure 6 illustrates the growth of CdSe as a function of temperature in a microwave reactor at 300 W and a fixed power of 160 W. The CdSe nanomaterials have well-defined excitonic features and QYs on the order of 74% consistent with previously published materials in the literature.<sup>34</sup> More importantly, these materials are combined at 50 °C (to maintain reaction liquidity), require no high-temperature injection step and no multiple injection for size focusing, and can be isolated within 30 s of initiating the reaction regardless of the desired size. It is clearly observed that a very narrow size distribution is maintained throughout the reaction for all sizes with no PL defect emission.

**InGaP Nanoparticle Formation.** Formation of III–V materials is notorious for its difficulty and required long reaction times (h). Microwave heating has been shown to be advantageous in such cases. In organometallic reactions in the microwave, superheating of the solvent and vessel pressurization has been shown to give rise to a 1000-fold increase in reaction rate.<sup>46</sup> More interestingly, it has been observed that when the polarity of the solvent is decreased (i.e. when the solvent becomes more transparent) for some synthesis, the observed reaction rate and product yield increase. This implies that there is a stronger microwave–material interaction in the more transparent solvents, giving rise to microwave-specific effects.<sup>47</sup>

The formation characteristics for InGaP nanoparticles by microwave heating are compared between a high-boiling,

(46) Mingos, D. M. P.; Baghurst, D. R. *Chem. Soc. Rev.* **1991**, *20*, 1–47.

(47) Loupy, A.; Perreux, L.; Liagre, M.; Burle, K.; Moneuse, M. *Pure Appl. Chem.* **2001**, *73*, 161–166.

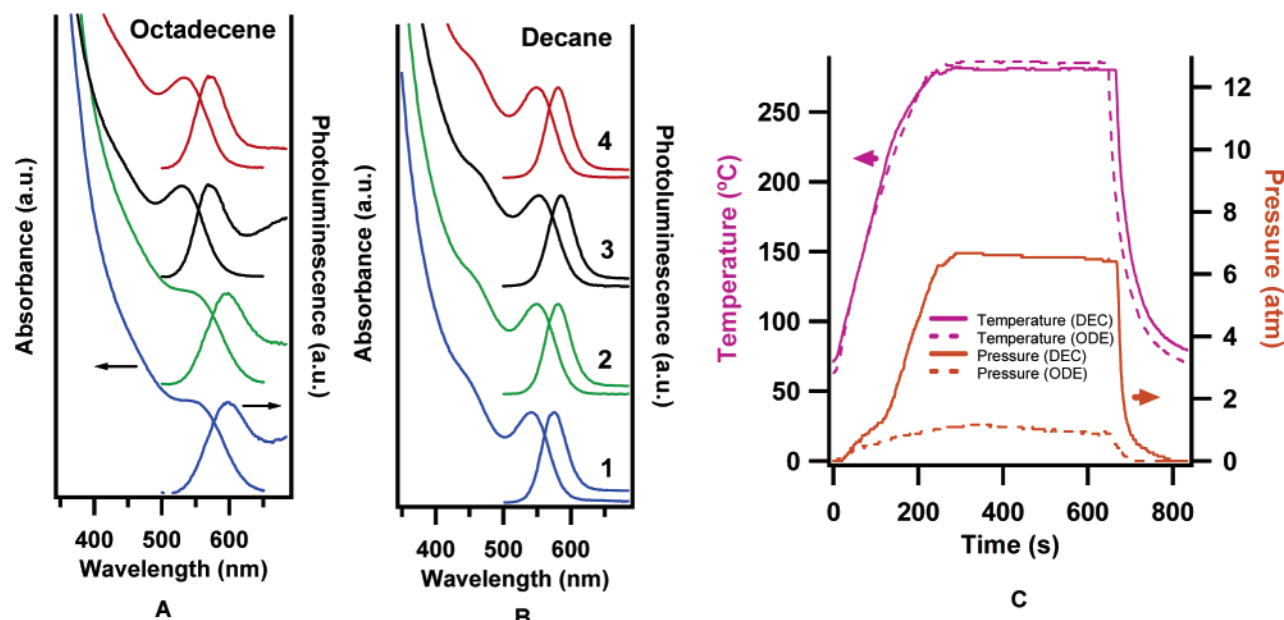


**Figure 7.** Growth characteristics of InGaP at 280 °C and 280 W in a high-boiling, noncoordinating solvent (A) octadecene (ODE) and a low-boiling (B) decane (DEC). The reaction time in both solvents was (B1) 30 s, (B2) 1 min, (B3) 3 min, and (B4) 7 min. (C) Temperature (°C) and pressure profiles (atm) of the reaction consisting of the high-boiling, ODE, and low-boiling, decane, noncoordinating solvents.

noncoordinating solvent ODE and a low-boiling solvent decane. ODE and other alkane and alkene noncoordinating solvents provide an ideal reaction system to study the effects of microwave–material interaction due to their relative transparency to the microwave field.

As seen in Figure 7A, the formation of InGaP in ODE under constant temperature and power shows a focusing of size distribution<sup>35</sup> with a reduction of size at longer reaction times during a reaction time from 30 s to 7 min. At 7 min, the size distribution and PL are maximized, when the applied power is 280 W and the reaction temperature is 280 °C. With time, the onset of the first exciton and the quality of the PL becomes more resolved with a final size of 4.0 nm. Inspection of the reaction at variable temperature ( $P = 280$  W,  $t = 7$  min) and variable power ( $T = 280$  °C,  $t = 7$  min) (Supporting Information Figure 4) suggests that while reaction temperature is critical for observing a clear excitonic feature ( $> 280$  °C), no effect on the excitonic feature is observed for power between 230 and 300 W with a fixed reaction temperature of 280 °C. Inspection of the PL is more informative. The QY increases steadily with increasing applied power from a value  $< 1\%$  ( $P = 230$  W) to a value of 4% at 300 W in ODE. While this number is low compared to CdSe, it is on the order of QY's measured for thermally grown InP samples isolated from reaction.<sup>48</sup> Following chemical etching in HF, as described in the literature, the QY increases to a maximum value of 68% due to removal of surface defects.<sup>49,50</sup>

The influence of reaction pressurization on the rate of growth and quality of materials for InGaP nanocrystals is clearly observed in Figure 7B. The same reaction carried out in decane rather than ODE produces astonishingly well-resolved excitonic features for InGaP of roughly the same size. It is clear that the

size remains nearly constant and that the size distribution becomes focused around 1 min (Figure 7B2) and remains constant up to 7 min. The PL quantum efficiency for the decane reaction ranges from 9% for a 30 s reaction to 15% for the 7 min reaction. This is the first report, to our knowledge, of quantum efficiencies of a chemically nonetched, un-size-selected III–V system that exhibits quantum efficiencies of this magnitude. Comparing the formation rate of InGaP in ODE and decane, it is apparent that the quality and rate is dramatically enhanced in decane. Chemical etching with HF produces QYs of the same level as the samples grown in ODE. This suggests that a reaction in superheated solvents overcomes local defect-driven minima in the reaction trajectory producing more narrowly sized and optically better materials.

Although no size dependent trends are observable for InGaP in either decane or ODE, the change in the absorption features and the PL properties are indicative of particle annealing and size focusing. Details on size dependence and optical properties of InGaP, InP, and InP/ZnS core shell prepared in the microwave will be reported in a future paper.<sup>51</sup> With increasing reaction temperature or applied power, the PL shows a loss of defect emission coupled to increased quantum efficiencies for the nanomaterials. These effects are more important in the ODE-grown materials, suggesting the reaction may be moderated by nanoparticle reconstruction or defect formation, such as vacancies or glide plane defects influencing the growth of these materials. Consistent with the experimental observations, at higher temperature or longer reaction times, particle annealing would be enhanced due to an increase in diffusion of the vacancies to the nanomaterial surface following a Boltzmann dependent diffusion process and the expectation of defect migration by Fick's law toward the surface of the nanomaterial. In contrast to the material formed in ODE, decane appears to promote a stronger coupling of the microwave–nanomaterial interaction. This is seen in the superheated decane reaction

(48) Lucey, D. W.; MacRae, D. J.; Furis, M.; Sahoo, Y.; Cartwright, A. N.; Prasad, P. N. *Chem. Mater.* **2005**, *17*, 3754–3762.  
 (49) Micic, O. I.; Nozik, A. J.; Lifshitz, E.; Rajh, T.; Poluektov, O. G.; Thurnauer, M. C. *J. Phys. Chem. B* **2002**, *106*, 4390–4395.  
 (50) Talapin, D. V.; Gaponik, N.; Borchert, H.; Rogach, A. L.; Haase, M.; Weller, H. *J. Phys. Chem. B* **2002**, *106*, 12659–12663.

(51) Unpublished results.

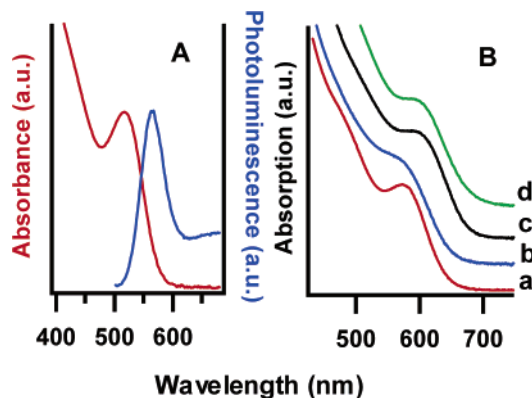


**Figure 8.** Absorbance and photoluminescence of InP in toluene (A). Absorbance of a series of InP nanoparticles is formed in the presence of ionic liquids at 280 °C for 15 min at 280 W (B): (a) as-prepared InP nanoparticles with no ionic liquid present, (b) InP with trihexyltetradecylphosphonium decanoate, (c) InP with trihexyltetradecylphosphonium bromide, and (d) InP with trioctylphosphine oxide.

compared with that of ODE (Figure 7C). When the reaction containing decane approaches 200 °C, the pressure increases rapidly until it is sustained at 6.2 atm for the duration of the reaction. It is observed from both reactions in ODE and decane that there is a rise in pressure at the onset of the reaction, suggesting that there is a volatile byproduct that is liberated as the nanoparticle reaches its maximum size. This is possibly a low-boiling organic that diffuses back into solution when the reaction is cooled.

**InP Nanoparticle Formation.** The influence of vacancies, defects, and surface energies on nanomaterial surfaces is apparent when the reaction conditions required for formation of InGaP and InP are compared. The InP materials exhibit a significantly longer reaction time for a maximum in the PL quantum efficiency to be observed. For growth of InP in ODE, the optimum reaction time was found to be 15 min at 280 °C with an applied power of 280 W (Figure 8Ba) without any additives. InP shows similar trends in material size distribution and optical quality with power, and temperature in analogy to the InGaP samples. The quantum efficiency of the as-prepared (non-HF-etched) InP material under optimal reaction condition is 4% with a value of 38% following HF etching.

The drastic increase in reaction time suggests that the surface in InGaP more easily anneals than the binary system. This is not surprising in that a defect ion has been observed to increase reaction rates in II–VI materials.<sup>52,53</sup> Alternatively, the enhanced rate for InGaP growth may be influenced by the formation of an In/Ga flux at the nanomaterial surface during the synthetic reaction. Burho et al. has suggested that InP grows at the interface of an In<sup>0</sup> droplet.<sup>54</sup> In this case the In/Ga flux may lower than the activation barriers in the reaction and the Ga would be expected to isolate at or near the nanoparticle surface. In fact, recent NMR and XPS studies suggest the Ga isolates at or near the surface (unpublished results). Continuing studies to elucidate the growth mechanism in low-boiling solvents and the influence of ionic liquids on the formation characteristics are ongoing in the laboratory.

Inspection of the influence of strong microwave absorbers (ILs and TOPO) on the growth of InP is a more complicated issue than for the II–VI materials, possibly due to interactions of the IL with the precursors. The observations are dependent on the nature of the IL (imidazolium vs phosphonium) and require further studies to fully elucidate the influence on the reaction mechanism on InP growth. In the presence of the 1-hexyl-3-methylimidazolium chloride IL, the nanomaterial precipitates to form an insoluble orange residue. This is presumably either a cluster or a small coordination complex, although clear identification of the product is still under investigation. When a phosphonium-based IL is added, such as trihexyltetradecylphosphonium decanoate or trihexyltetradecylphosphonium bromide, no precipitation is observed; however, the onset of the first exciton is shifted relative to the reaction carried out in the absence of the IL (Figure 8B) and shows no visible PL. The addition of TOPO results in a broadening of the absorption feature and has substantially lower quantum efficiency. In both additive cases (IL or TOPO) etching does not produce a substantial improvement of the PL performance over the reaction carried out in the absence of the additive. In addition, additives appear to broaden the size distribution. While additives have a marked effect on nanoparticle growth and quality, the effect is not advantageous in the III–V family. At this time the negative influence on quality would only be speculative in the absence of a well-understood reaction mechanism.

## Conclusion

Dielectric heating is advantageous to the formation of nanocrystals. High operating powers and temperatures in the MW cavity allow nearly monodisperse high-quality nanomaterials with QYs up to 74% to be rapidly generated in under 20 min. The use of the microwave eliminates thermal gradients by volumetric heating, eliminates the need for high-temperature injection for size focusing, and is scalable for commercialization. The influence of additives, power, temperature, and time is demonstrated for both the II–VI and III–V nanocrystalline systems. While the exact nature of the microwave-specific effect is difficult to define for these materials due to their complex reaction trajectories, it is clear that the method can be tuned to optimize reaction conditions for specific materials. For instance, addition of ionic liquids that raise the rate of heating improves the growth rate for CdSe, while higher reaction pressures enhance the formation of III–V materials. This suggests that the nature of the transition states for growth in these systems is different and may be influenced by surface or defect formation.

The observed reaction rate enhancement and size focusing in nanocrystalline materials grown under dielectric heating conditions may arise from elevated reactant temperatures due to selective heating coupled to rapid cooling through thermalization. Because, in the microwave, the reactions are volumetrically heated, thermal gradients tend to be minimized, which results in a more uniform reaction. Selective heating arises from the relative differences in solvent and reactant dielectric constants. This means that the microscopic temperature instantly rises when the microwave field is applied. The implication is that the internal temperature of the reaction at or near the nanoparticle surface is significantly higher than what is detected by the infrared detector which ultimately reads the vessel temperature. Rapid thermalization to focus the nanoparticle size

(52) Hanif, K. M.; Meulenberg, R. W.; Strouse, G. F. *J. Am. Chem. Soc.* **2002**, *124*, 11495–11502.

(53) Treadway, J. A.; Zehnder, D. A. U. S. Patent 20030017264, 2003.

(54) Trentler, T. J.; Goel, S. C.; Hickman, K. M.; Viano, A. M.; Chiang, M. Y.; Beatty, A. M.; Gibbons, P. C.; Burho, W. E. *J. Am. Chem. Soc.* **1997**, *119*, 2172–2181.

is achieved because of the high surface-to-volume ratio of nanoparticles below 7 nm coupled with the fact that they are colloidally suspended in solution. This tends to enhance the thermal field within the reaction matrix regardless of which direction the heat is transferred, either from particle to solvent or solvent to particle.

In addition the observations in this manuscript indicate that additives or pressurization can accelerate growth and suggests vacancy, defect, or reconstruction processes influence the growth behavior of these materials along the reaction trajectory. This synthetic strategy can be tailored to a host of nanomaterials to enhance the efficiency of the nanomaterial discovery and the optimization of nanostructured materials. Moreover, the III–V nanomaterials and the harsh environment and high temperatures needed for growth is no longer a limiting factor governing industrial scalability of such materials. The ability to control the reaction with microwaves offers a more environmental approach to colloidal semiconducting nanoparticles. The demonstration of microwave techniques effectively automates

the synthetic process and, more importantly, demonstrates the use of a continuous flow microwave reactor for nanoparticle formation.

**Acknowledgment.** We would like to thank the CEM Corp. for performing the necessary modifications to the reactor cavity and magnetron, as well as the extended use of the Discover microwave and Voyager stopped-flow microwave stations. We would also like to thank Tomohide Murase, Takeshi Ohtsu, and Itaru Kamiya for helpful discussions.

**Supporting Information Available:** Complete reference 12, pXRD and TEM of InGaP nanoparticles (Supporting Information Figures 1 and 2), and a comparison of the absorption and photoluminescence of CdSe nanoparticles with and without the ionic liquid added (Supporting Information Figure 3) (pdf). This material is available free of charge via the Internet at <http://pubs.acs.org>.

JA052463G